Lab on a Chip

View Online
Dynamic Article Links

Cite this: *Lab Chip*, 2011, **11**, 3162

www.rsc.org/loc

PAPER

Double-emulsion drops with ultra-thin shells for capsule templates†

Shin-Hyun Kim,[a] Jin Woong Kim,[b] Jun-Cheol Cho[c] and David A. Weitz*[a]

Received 20th May 2011, Accepted 14th July 2011
DOI: 10.1039/c1lc20434c

We introduce an emulsification technique that creates monodisperse double-emulsion drops with a core–shell geometry having an ultra-thin wall as a middle layer. We create a biphasic flow in a microfluidic capillary device by forming a sheath flow consisting of a thin layer of a fluid with high affinity to the capillary wall flowing along the inner wall of the capillary, surrounding the innermost fluid. This creates double-emulsion drops, using a single-step emulsification, having a very thin fluid shell. If the shell is solidified, its thickness can be small as a hundred nanometres or even less. Despite the small thickness of this shell, these structures are nevertheless very stable, giving them great potential for encapsulation. We demonstrate this by creating biodegradable microcapsules of poly(lactic acid) with a shell thickness of a few tens of nanometres, which are potentially useful for encapsulation and delivery of drugs, cosmetics, and nutrients.

Introduction

Double-emulsion drops or drops in drops have been used as templates to produce many types of microcapsules; great control of their production can be achieved through the use of microfluidic devices.[1,2] The robustness of final capsule structure can be further increased through the use of core–shell geometry where the middle phase of the double-emulsion drops is solidified, ensuring that a solid layer separates the inner compartment from the outer fluid. This solidification can be achieved in three distinct ways; solvent evaporation,[3,4] polymerization,[5–7] or dewetting of the middle phase onto the surface of the innermost drop.[8–10] Evaporation of the middle phase physically consolidates any colloids, polymers or smaller emulsion drops within the shell, resulting in a porous membrane with a size-selective permeability.[3,4] Alternatively, polymerization of a monomer solution in the middle phase produces microcapsules whose membranes are composed of crosslinked polymers.[5–7] The dewetting of the amphiphile-laden middle phase creates liposomes or polymersomes with molecular bilayers.[8–10] However, preparation of a double-emulsion drop with highly viscous organic solvents remains a challenge; for example, organic solvents containing high concentrations of colloids, monomers, or polymers, which are commonly required to prepare functional microcapsules, are very difficult to use in fabrication of the structures. Furthermore, the interfacial energies of double-emulsion drops can frequently lead to coalescences and merging of innermost drops with the continuous phase before the consolidation is fully completed. One possible means to significantly increase the stability of such double-emulsion drops is through the reduction of the thickness of the middle phase; if it is very thin, the lubrication effect greatly slows the migration of the inner drop to the outer wall, markedly improving the stability. However, creation of such a thin middle layer is challenging using capillary microfluidic approaches. There has been one attempt to create such double-emulsion structures using PDMS devices with sequential emulsification, where much of the middle layer is removed during the second emulsification step; however, these devices rely on delicate control of both flow and the wettability, making robust operation difficult.[11] Thus, a method that combines the ease of fluid flow control and the robustness of capillary microfluidic devices to create the double-emulsion drops with a very thin shell in a one-step emulsification process remains an important yet unmet need.

In this article, we report a novel and practical approach to make monodisperse double-emulsion drops with an ultra-thin middle layer using single-step emulsification in a capillary microfluidic device. We create a biphasic flow consisting of a sheath of one fluid flowing along the capillary wall and surrounding a second fluid flowing through the center of the capillary. This biphasic flow forms double-emulsion drops that have core–shell structure with a very thin outer wall. This technique enables the preparation of double-emulsion drops with highly viscous organic solvents, facilitating the formation of functional microcapsules with an ultra-thin membrane. We exploit these features to make biodegradable microcapsules with a shell thickness of a few tens of nanometres using evaporation-induced solidification in water-in-oil-in-water (W/O/W) double-emulsion drops.

[a]*School of Engineering and Applied Sciences and Department of Physics, Harvard University, Cambridge, Massachusetts, USA. E-mail: weitz@seas.harvard.edu; Tel: +1-617-495-3275*
[b]*Department of Applied Chemistry, Hanyang University, Ansan, South Korea*
[c]*Amore-Pacific Co. R&D Center, Yongin, South Korea*

† Electronic supplementary information (ESI) available: Figures for O/W/O double-emulsion drops and movies for W/O/W double-emulsion generation in the continuous and discontinuous modes. See DOI: 10.1039/c1lc20434c

Results and discussion

A biphasic flow confined in a capillary

Two immiscible fluids which flow coaxially and simultaneously through a single capillary can exhibit two distinct flow patterns, consisting of either a coaxial jet or a stream of drops of one fluid in the second. A jet of one liquid in the second is typically unstable to the Rayleigh–Plateau instability which causes a breakup of the jet into drops; this instability can be suppressed by confining the coaxial flow.[12,13] Further control over the fluid flow can be achieved by exploiting the affinity of the fluid to the capillary; the fluid with higher affinity to the wall will flow along it whereas the second fluid will flow through the center of the capillary. Because of the affinity to the wall, the thickness of the outer fluid can be very thin. We employ such a biphasic flow, using either a stable jet or plug-like drops, to produce double-emulsion drops. By controlling the thickness of the fluid with high affinity to the wall, we are able to produce double-emulsion drops with an ultra-thin middle layer using a one-step emulsification process. To make W/O/W double-emulsion drops, we use a capillary microfluidic device comprised of a hydrophobic tapered injection capillary inserted into a second square capillary (AIT glass) whose inner dimension is the same as that of the outer diameter of the injection capillary, which is typically 1 mm, as schematically illustrated in Fig. 1a. We use *n*-octadecyltrimethoxy silane (Aldrich) to make the capillary wall hydrophobic. In addition, a small tapered capillary is inserted into the injection capillary to simultaneously inject a second immiscible fluid, as shown in Fig. 1a. Another circular capillary is inserted into the square capillary at the other side to confine the flow near the injection tip, thereby increasing the flow velocity; this is coated by 2-[methoxy(polyethyleneoxy)propyl]trimethoxy silane (Gelest, Inc.) to make the capillary wall hydrophilic. We inject a 25 wt% aqueous solution of poly(ethylene glycol) (PEG, M_w 6000) through the small tapered capillary to form the inner drops. We use hexadecane with 1 wt% SPAN 80 for the middle fluid and inject this through the injection capillary. The continuous phase is a 10 wt% aqueous solution of poly(vinyl alcohol) (PVA, M_w 13 000–23 000) which is injected through the square capillary as shown in Fig. 1a.

The inner diameter of the injection capillary significantly influences the flow patterns. When employing an injection capillary with an inner diameter of 580 μm (World precision instruments, Inc., 1B100-6), we observe formation of water drops in the hexadecane within the injection capillary for a wide range of flow rates. Even when the volumetric flow rate of the inner phase is as much as a factor of 4 larger than that of the middle phase and their linear flow velocities are quite high, a train of plug-like drops are observed as shown in Fig. 1b. These plug-like drops are emulsified at the tip of the injection capillary, resulting in monodisperse double-emulsion drops with an ultra-thin middle layer; however there is excess oil in the middle phase which is not incorporated into the emulsion drops, but instead form large independent oil blobs between double-emulsion drops. This discontinuous generation of double-emulsion drops is shown in Fig. 1c and in the first part of the Movie S1 in the ESI†. In contrast, a stable water jet is formed in the injection capillary when the inner diameter is 200 μm (AIT glass) as shown in Fig. 1d; this is emulsified at the tip in a continuous fashion, resulting in monodisperse double-emulsion drops, as shown in Fig. 1e and the second part of the Movie S1†. As the inner diameter of the capillary decreases, there is a higher degree of interfacial confinement, thereby reducing deformation of the interface and making a more stable jet.

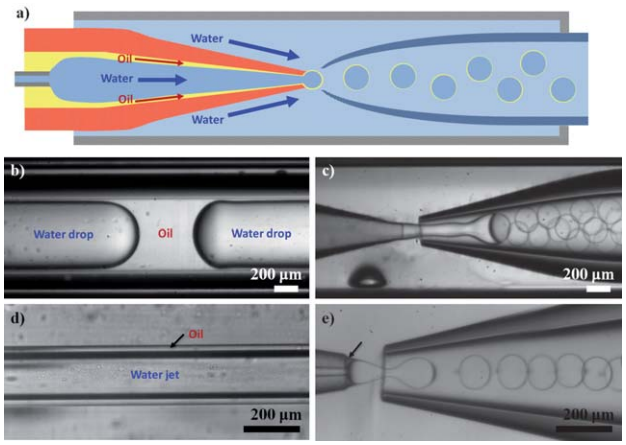

Fig. 1 (a) Schematic illustration of the microfluidic device for preparation of double-emulsion drops with an ultra-thin shell. (b and c) Optical microscope images showing flow of water drops in the injection capillary with an inner diameter of 580 μm and their emulsification at the tip of the injection capillary, where flow rates of inner (Q_1), middle (Q_2), and continuous (Q_3) phases are maintained at values of 4000 μl h^{-1}, 1000 μl h^{-1}, and 5500 μl h^{-1}, respectively. (d and e) Optical microscope images showing a stable water jet in the injection capillary with an inner diameter of 200 μm and its emulsification at the tip of the injection capillary, where Q_1, and Q_2, and Q_3 are maintained at values of 2500 μl h^{-1}, 500 μl h^{-1}, and 8000 μl h^{-1}, respectively.

Emulsification of biphasic flow

The flow rates of inner (Q_1), middle (Q_2), and continuous (Q_3) phases each influence the flow patterns in the injection capillary and the double-emulsion generated, as summarized in Fig. 2a. At any given Q_2, a stable water jet is formed in the 200 μm diameter injection capillary for sufficiently large Q_1, as denoted by blue circles in Fig. 2a and in the top image of Fig. 2b. However, a double-emulsion is not always produced by the jet; high inertia of the inner stream at high Q_1 causes a leakage of the inner stream into the continuous phase near the tip of the injection capillary, as denoted by the violet-colored region in Fig. 2a. In contrast, for Q_1 in the region denoted by blue color, double-emulsion drops are generated continuously in either the jetting or the dripping modes.[14] For high Q_1, the jet flows through the orifice of the collection capillary and then breaks into double-emulsion drops at the end of the jet, as shown in Fig. 2c. In contrast, for low Q_1, the jet is emulsified in the dripping mode, near the tip of the injection capillary, as shown in Fig. 2d. As Q_1 is further reduced, as denoted by the green region, the jet becomes unstable and exhibits fluctuations of the interface but does not breakup, as shown in the middle image of Fig. 2b. A further reduction of Q_1, as denoted by the red region, yields plug-like water drops in the injection capillary as shown in the bottom image of Fig. 2b; this produces a discontinuous flow of

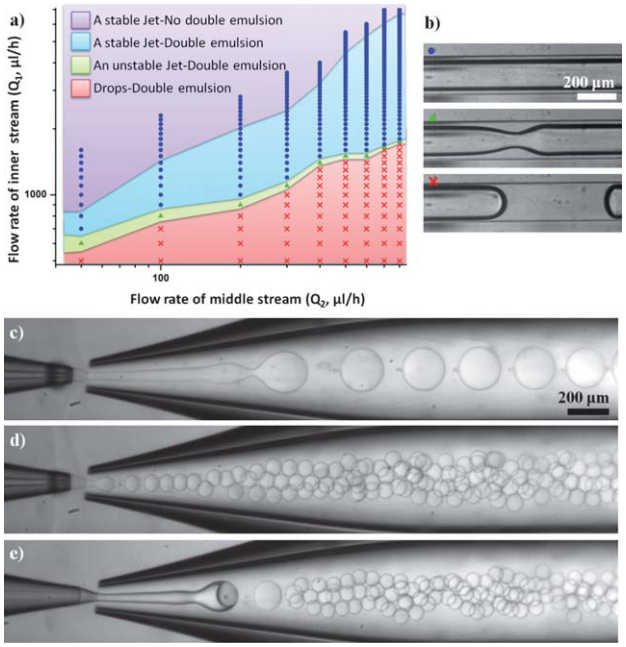

Fig. 2 (a and b) Flow behavior as a function of Q_1 and Q_2, where Q_3 is maintained at 4500 μl h^{-1}. Circles, triangles, and crosses denote a stable jet, an unstable jet and drops, respectively, as shown in (b). The range of stability is quite large. (c–e) Optical microscope images showing (c) the continuous jetting, (d) the continuous dripping, and (e) the discontinuous dripping modes of double-emulsion generation, where Q_1 is (c) 1200 μl h^{-1}, (d) 800 μl h^{-1}, and (e) 400 μl h^{-1}, respectively and Q_2 and Q_3 are maintained at 100 μl h^{-1} and 4500 μl h^{-1}, respectively.

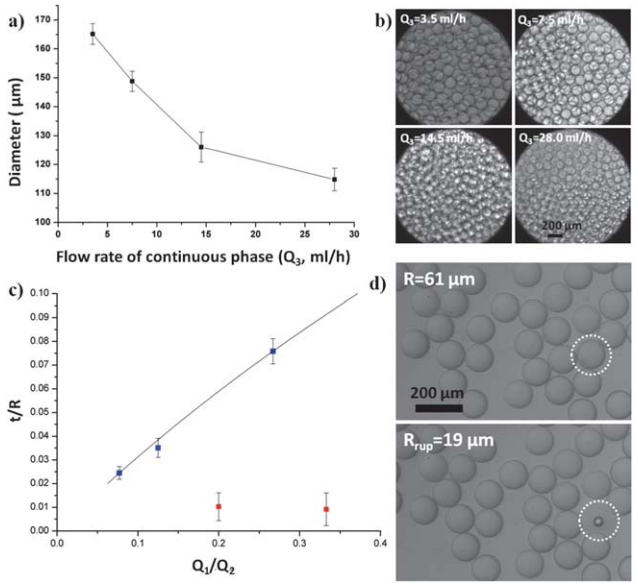

Fig. 3 (a) Size of the double-emulsion drops as a function of Q_3. (b) Optical microscope images of monodisperse double-emulsion drops prepared at the values of Q_3 denoted on images. (c) Relative thickness of shell to radius of the double-emulsion drops (t/R) as a function of Q_1/Q_2. Blue and red squares correspond to t/R of the double-emulsion drops prepared by the continuous jetting or dripping modes and the discontinuous dripping mode, respectively. (d) Optical microscope images showing rupturing of a double-emulsion drop, resulting in formation of a single emulsion drop as denoted by the dotted circles.

double-emulsion drops in the dripping mode, as shown in Fig. 2e. The generation of double-emulsion drops in the continuous jetting, the continuous dripping, and the discontinuous dripping modes is explicitly displayed in Movie S2 in the ESI†.

We also produce O/W/O double-emulsion drops in the same manner. Using a microcapillary device with the same geometry but with the hydrophilic and hydrophobic surface modifications reversed, we prepare double-emulsion drops of silicone oil (AR 20)/1 wt% aqueous solution of Pluronic F108 (BASF)/2 wt% silicone oil (AR 20) of DC749 (Dow Corning), which are shown in Fig. S1 in the ESI†.

Diameter and shell thickness of double-emulsion drops

When operating in the dripping mode, drop generation is governed by two competing forces: the capillary force that holds the drop to the tip and the drag force that pulls the drop downstream.[15] Therefore, we can also control the size of the double-emulsion drops through Q_3, which sets the drag force. When we increase Q_3, the diameter of the double-emulsion drops decreases as shown in Fig. 3a and b. The resultant double-emulsion drops remain highly monodisperse, and their diameters have a coefficient of variation in the range of 1.0–1.9%.

The thickness, t, of the middle layer of the double-emulsion drops is too small to measure directly from an optical microscope image. Therefore, we rupture the double-emulsion drops to form a single emulsion drop and determine the shell thickness from the radius of this single emulsion drop (R_{rup}) and that of the original double-emulsion drop (R):

$$t = R - \left(R^3 - R_{rup}^3\right)^{1/3} \quad (1)$$

For example, two optical microscope images shown in Fig. 4d exhibit rupturing of a double-emulsion drop, resulting in formation of a single emulsion drop as denoted by the dotted circles; to rupture them, we place the double-emulsion drops on top of a glass slide, and tap it several times. For these two images, $R = 61$ μm and $R_{rup} = 19$ μm, and we use these values to calculate $t = 620$ nm, where the approximately 10% uncertainty of the thickness results from the limits of the resolution of the optical microscope. In the same fashion, we calculate the thickness of the middle layer of double-emulsion drops which are produced at each values of Q_1/Q_2 and plot the results in Fig. 3c; blue squares correspond to the thicknesses of the middle layer of the double-emulsion drops prepared in either the continuous jetting or dripping modes, while red squares correspond to those of the double-emulsion drops prepared in the discontinuous dripping mode. The blue dots are in good accord with the solid line which describes the mass balance equation:

$$\frac{t}{R} = 1 - \left(1 + \frac{Q_1}{Q_2}\right)^{1/3} \quad (2)$$

In contrast, the discontinuous dripping mode always produces double-emulsion drops with very small values of t/R, regardless of flow rates. We attribute this to the very small volume of oil between the plug-like water drop and the inner wall of the injection capillary, which forms the middle layer of the

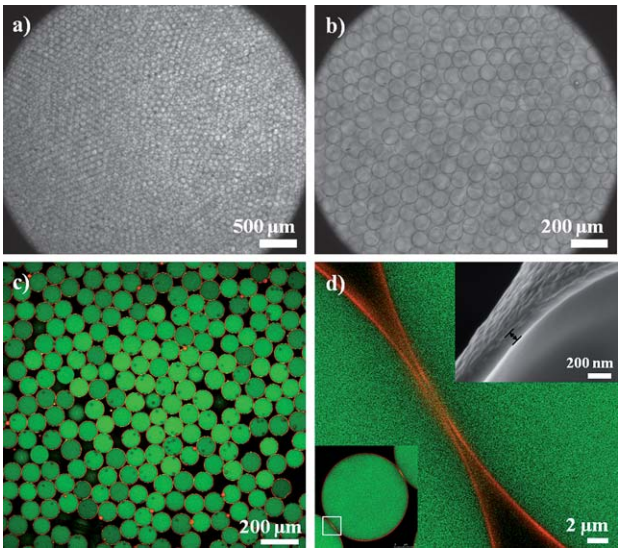

Fig. 4 (a and b) Optical microscope images of monodisperse double-emulsion drops before consolidation of the middle phase. (c and d) Confocal microscope images of microcapsules with a poly(lactic acid) membrane. A scanning electron microscope image in the inset of (d) shows a cross-section of the membrane.

double-emulsion drops. Most of the injected oil is situated in the large oil blobs which form between the double-emulsion drops. Although the discontinuous mode produces both monodisperse double-emulsion drops with an ultra-thin shell and large oil drops, separation of the double-emulsions from the mixture is easily accomplished by exploiting the density difference between them, which leads to differences in their terminal velocities; the average density of the double-emulsion drops with an ultra-thin shell is essentially identical to that of an aqueous core whereas the oil drops have the density of the oil solution. Therefore, both the continuous and discontinuous dripping modes are useful for production of microcapsules with an ultra-thin membrane.

Biodegradable microcapsules from double-emulsion drops

Our approach can be used to make double-emulsion drops with fluids having a wide range of viscosities; thus, highly concentrated organic solutions of polymers can be used for the middle phase. Moreover, an ultra-thin middle layer provides stability to the double-emulsion drops, preventing coalescence of the innermost drop with the continuous fluid; such stability is otherwise difficult to achieve with a larger thickness. We attribute the enhancement of stability to the significantly increased drag force on the innermost drop because the very thin width of the middle phase puts the fluid in the lubrication regime. For example, the migration velocity of an inner drop that is 98 μm in diameter is reduced by a factor of 10^5 for an outer shell that is 100 μm in diameter in comparison with an inner drop that is 50 μm in diameter for the same size of outer shell.[16,17] Although the migration velocity decreases as an inner drop approaches the interface of an outer drop in both cases, a very thin middle phase puts the fluid of the whole middle layer into the lubrication regime, whereas a thick middle phase puts only the fluid of the thinnest region into the lubrication regime. Therefore, even the migration velocity approaching the interface of an outer drop is significantly reduced for an ultra-thin middle layer in comparison with that for a thick middle layer. In addition, emulsification of either a jet or plug-like drops provides a higher frequency for double-emulsion-drop generation, making it comparable with the frequency for single-emulsion generation.

To illustrate these advantages, we prepare polymeric microcapsules whose membrane is made of biodegradable polymer, poly(lactic acid) (PLA, M_w 15 000). We form inner drops with a 10 wt% aqueous solution of PVA containing a green dye, 8-hydroxyl-1,3,6-pyrenetrisulfonic acid, trisodium salt. For the middle phase, we use a solution of PLA at 20 wt% in toluene containing a red dye, nile red, and for the continuous phase, we use a 3 wt% aqueous solution of PVA. We generate approximately 1000 drops per second by employing the discontinuous dripping mode, resulting in highly monodisperse double-emulsion drops, as shown in Fig. 4a and b. The average density of the double-emulsion drops is larger than the continuous phase; thus, although large toluene blobs are also generated, they are easily separated from the double-emulsion drops since their density is lower than that of the continuous phase. The suspension of drops is held at 65 °C for 2 hours to evaporate toluene from the middle layer; this leads to the consolidation of the middle layer to a polymeric membrane, as shown in the confocal microscope images of Fig. 4c and d. At the maximum magnification of the confocal microscope, we observe that the thickness of the shell is less than 500 nm, as seen in Fig. 4d. We determine the thickness of the membrane to be 80 nm from the scanning electron microscope image shown in the inset of Fig. 4d. This value is reasonable when we consider the significant shrinkage of the thickness of the middle layer from hundreds of nanometres during the consolidation process.

The membrane material is PLA, which is biodegradable due to hydrolysis of ester groups in its chain.[18] Therefore the microcapsules can dissociate and release materials encapsulated in the aqueous core. All capsules dispersed in a 3 wt% aqueous solution of PVA initially have green dye in the core, as shown in Fig. 4c; the capsules release the dye as the PLA degrades. Within 71 days, all capsules rupture as shown in the bottom image of Fig. 5a. The fraction of unruptured microcapsules depends on time as shown

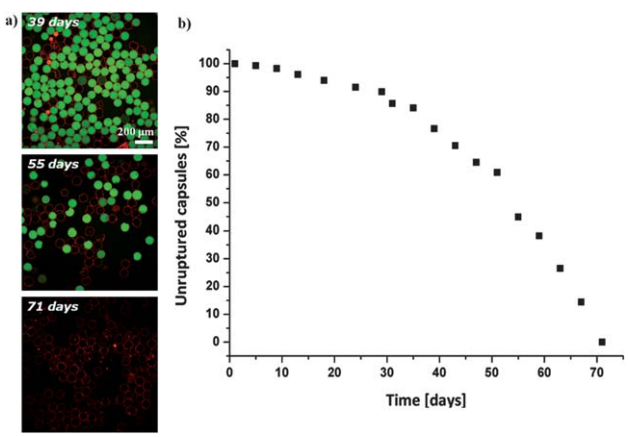

Fig. 5 (a) Confocal microscope images of microcapsules taken at the times, measured from capsule preparation, denoted in the images. (b) Fraction of unruptured capsules as a function of time.

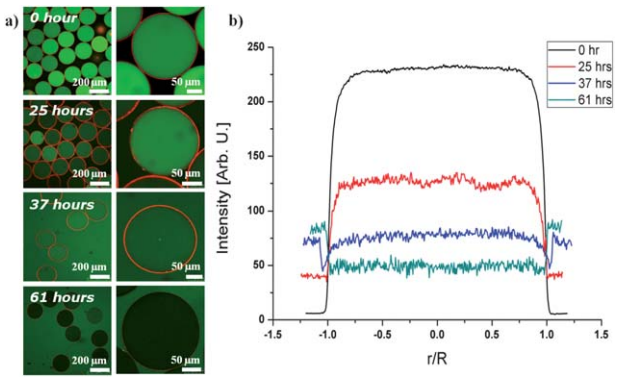

Fig. 6 (a) Confocal microscope images of microcapsules dispersed in water, taken at the times, measured from capsule preparation, denoted in the images. (b) Cross-section of the fluorescent intensity of the green dye in the microcapsules at the times denoted in the figure.

in Fig. 5b. In contrast, capsules release encapsulants quickly when they experience a high osmolarity difference between the core and the continuous phase. When the capsules are dispersed in distilled water, the capsules start to release the dye within a day. Because the osmolarity in the core is higher by 100 mOsm, the capsules are inflated by the inward flow of water; this leads to generation of pores on the membrane, as confirmed by the decrease in the dye concentration in the core. Thus, the intensity of green dye in the core decreases while the intensity of that in the continuous phase increases, as shown in confocal microscope images of Fig. 6a and the cross-sections of the fluorescent intensity of the green dyes of Fig. 6b. Ultimately, at 61 hours, all the interior dye has escaped; the lower intensity in the core as compared to that in the continuous phase results from absorption of the green light emitted by interior dye by red dye in the membrane.

Conclusions

We produce monodisperse double-emulsion drops with an ultra-thin middle layer through a one-step emulsification process using a biphasic flow, confined in a microcapillary, operated in either a stable jet or in a flow of drops. This technique enables production of double-emulsion drops even with highly viscous fluids; moreover the thickness of the shell can be reduced to submicron scales, which is difficult to achieve with any other approach. The very thin middle layer confers high stability to the double-emulsion drops, enabling high frequency drop generation while preventing rupturing during consolidation thus facilitating creation of microcapsules with an ultra-thin membrane of as little as a few tens of nanometres thick. This microfluidic approach should be useful for encapsulation and delivery of active materials such as drugs, cosmetics, and nutrients. Furthermore, the resultant microcapsules with their ultra-thin membranes can serve as model systems for studies of buckling phenomena of thin membranes[19] and for studies of phase behavior of polymer blends or block-copolymers that are spatially confined.[20]

Acknowledgements

This work was supported by Amore-Pacific, the NSF (DMR-1006546) and the Harvard MRSEC (DMR-0820484).

Notes and references

1 S. Okushima, T. Nisisako, T. Torii and T. Higuchi, *Langmuir*, 2004, **20**, 9905–9908.
2 A. S. Utada, E. Lorenceau, D. R. Link, P. D. Kaplan, H. A. Stone and D. A. Weitz, *Science*, 2005, **308**, 537–541.
3 S. W. Choi, Y. Zhang and Y. N. Xia, *Adv. Funct. Mater.*, 2009, **19**, 2943–2949.
4 D. Lee and D. A. Weitz, *Adv. Mater.*, 2008, **20**, 3498–3503.
5 Y. Hennequin, N. Pannacci, C. P. de Torres, G. Tetradis-Meris, S. Chapuliot, E. Bouchaud and P. Tabeling, *Langmuir*, 2009, **25**, 7857–7861.
6 S. H. Kim, S. J. Jeon and S. M. Yang, *J. Am. Chem. Soc.*, 2008, **130**, 6040–6046.
7 Z. H. Nie, S. Q. Xu, M. Seo, P. C. Lewis and E. Kumacheva, *J. Am. Chem. Soc.*, 2005, **127**, 8058–8063.
8 R. C. Hayward, A. S. Utada, N. Dan and D. A. Weitz, *Langmuir*, 2006, **22**, 4457–4461.
9 E. Lorenceau, A. S. Utada, D. R. Link, G. Cristobal, M. Joanicot and D. A. Weitz, *Langmuir*, 2005, **21**, 9183–9186.
10 H. C. Shum, J. W. Kim and D. A. Weitz, *J. Am. Chem. Soc.*, 2008, **130**, 9543–9549.
11 D. Saeki, S. Sugiura, T. Kanamori, S. Sato and S. Ichikawa, *Lab Chip*, 2010, **10**, 357–362.
12 P. Guillot, A. Colin and A. Ajdari, *Phys. Rev. E: Stat., Nonlinear, Soft Matter Phys.*, 2008, **78**, 016307.
13 P. Guillot, A. Colin, A. S. Utada and A. Ajdari, *Phys. Rev. Lett.*, 2007, **99**, 104502.
14 A. S. Utada, A. Fernandez-Nieves, H. A. Stone and D. A. Weitz, *Phys. Rev. Lett.*, 2007, **99**, 094502.
15 P. B. Umbanhowar, V. Prasad and D. A. Weitz, *Langmuir*, 2000, **16**, 347–351.
16 J. Happel and H. Brenner, *Low Reynolds Number Hydrodynamics: with Special Applications to Particulate Media*, Kluwer, 1983.
17 L. S. Mok and K. Kim, *J. Fluid Mech.*, 1987, **176**, 521–531.
18 J. M. Anderson and M. S. Shive, *Adv. Drug Delivery Rev.*, 1997, **28**, 5–24.
19 E. Katifori, S. Alben, E. Cerda, D. R. Nelson and J. Dumais, *Proc. Natl. Acad. Sci. U. S. A.*, 2010, **107**, 7635–7639.
20 J. W. Shim, S. H. Kim, S. J. Jeon, S. M. Yang and G. R. Yi, *Chem. Mater.*, 2010, **22**, 5593–5600.

